

Journal of Astronomical Telescopes, Instruments, and Systems

AstronomicalTelescopes.SPIEDigitalLibrary.org

Aerodynamic modeling in dome seeing study of the 2.16-m telescope

Taoran Li
Jianfeng Tian
Jianfeng Wang
Xiaojun Jiang
Zhigang Hou
Hongbin Li

SPIE.

Taoran Li, Jianfeng Tian, Jianfeng Wang, Xiaojun Jiang, Zhigang Hou, Hongbin Li, "Aerodynamic modeling in dome seeing study of the 2.16-m telescope," *J. Astron. Telesc. Instrum. Syst.* **5**(2), 024011 (2019), doi: 10.1117/1.JATIS.5.2.024011.

Aerodynamic modeling in dome seeing study of the 2.16-m telescope

Taoran Li,^{a,*} Jianfeng Tian,^a Jianfeng Wang,^{a,b} Xiaojun Jiang,^{a,b} Zhigang Hou,^a and Hongbin Li^a

^aNational Astronomical Observatories Chinese Academy of Sciences, Key Laboratory of Optical Astronomy, Beijing, China

^bUniversity of Chinese Academy of Sciences, Beijing, China

Abstract. Aerodynamic analysis is a crucial part of evaluating dome seeing, which is one of the main factors affecting telescope image quality. Due to the large volume and high heat quantity inside the dome, dome seeing is a common issue. To characterize the thermodynamic performance of the 2.16-m telescope at the Xinglong Observatory, we describe computational fluid dynamic analyses for modeling the effects of passive ventilation as part of a preliminary study for a dome venting system. The aerodynamic modeling is built based on the structures of telescope and enclosure. In addition, the distribution of the temperature and the airflow around the enclosure are presented in several simulations with different slit orientations, including various wind–telescope relative azimuth angles. The airflow distribution was studied for two cases. The temperature and turbulent contour maps show that the current passive ventilation can cause turbulence and influence the accuracy of the image. The dome seeing is estimated using a postprocessing analysis based on the mechanical turbulence and temperature variations along the optical path. The results of dome seeing gave a suggestion of venting strategy. © The Authors. Published by SPIE under a Creative Commons Attribution 4.0 Unported License. Distribution or reproduction of this work in whole or in part requires full attribution of the original publication, including its DOI. [DOI: [10.1117/1.JATIS.5.2.024011](https://doi.org/10.1117/1.JATIS.5.2.024011)]

Keywords: 2.16-m telescope; dome; computational fluid dynamics; thermal modeling.

Paper 18129 received Dec. 26, 2018; accepted for publication May 8, 2019; published online May 27, 2019.

1 Introduction

The 2.16-m telescope, built in 1989, located at Xinglong Observatory, is an English equatorial mount telescope, with a primary mirror of diameter 2.16 m.¹ It has a large hemisphere dome with a diameter of 23 m and a height of 15 m. The rotating dome lies on a cylindrical wall comprising three layers: 1-mm aluminum sheet layer, air layer, and bearing wall. Both sides of the bearing wall are a 150-mm insulating layer. The 2.16-m telescope and a sectional drawing of the three-layer cylindrical wall are represented in Figs. 1 and 2, respectively.

Due to the large volume of the dome (~ 5600 m³) and high heat capacity inside the dome, several small exhaust fans could not balance the heat around the telescope. The wind coming from the 5-m-wide dome slit may cause air turbulence inside the dome. The accuracy and quality of images delivered by the telescope are adversely affected by dome seeing. Dome venting is an essential part of dome design. It could promote air circulation and reduce the dome seeing effect. Adding a series of large openings, “vents,” in the skin of the dome is an effective method to achieve the thermal and aerodynamic requirements for astronomical observations.

Efforts to improve the performance of the dome have been done from the 2010s. In 2011, the ventilation system was changed from blow to exhaust. These exhaust fans are triggered by temperature difference inside and outside the dome, whereas the old version was started-up by timing control. After a long period of time, the outside surface of the dome was peeling off. The dome was repainted with a new metal structural nanocoating in 2012. The reflectances in visible and thermal radiation of the coatings are larger than 98% and 86%, respectively. Earlier data showed that the dome repainting had an improvement on

the temperature difference by reducing the temperature inside the dome during daylight.

This paper describes the results of computational fluid dynamics (CFD) analyses of 2.16-m domes with different wind-slit angles, to characterize the thermodynamic performance of the 2.16-m telescope. The dome seeing is calculated using the temperature profiles along the optical path provided by CFD. The CFD analyses are aimed to estimate the aerodynamic performance of 2.16-m telescope and provide suggestions for a future dome venting upgrade.

2 Computational Fluid Dynamics Analysis

2.1 Telescope and Dome Simplification

The original model of 2.16-m telescope–dome contains tiny parts and complex shapes that can increase simulation time and are not necessary. Therefore, the mechanical model should be simplified (e.g., removing the screws and reconstructing the top end assembly as an annular part).

The simplified CFD model has five basic components, as shown in Fig. 3:

1. Dome
2. Mount
3. Simplified telescope structure (top end, M2, center box, M1)
4. Vents (for vented case)
5. Fluid domain (air).

The altitude of 2.16-m telescope is 891 m above the sea level. The height of the total building and cylindrical wall are 35 and 19 m, respectively. The rotating dome is 15-m tall and with a

*Address all correspondence to Taoran Li, E-mail: litaoran@bao.ac.cn

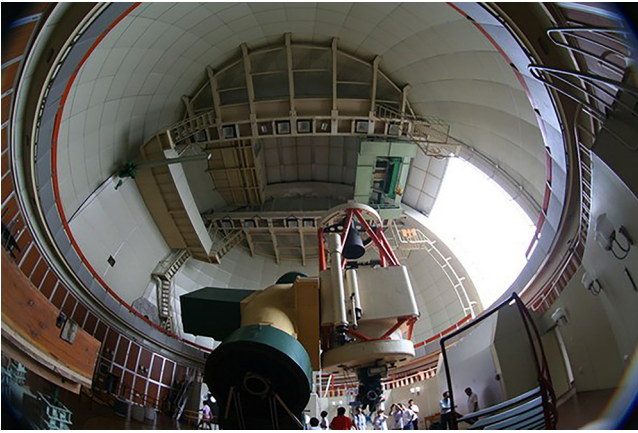


Fig. 1 2.16-m telescope and dome from a fisheye camera, credit: Chao Zhang.

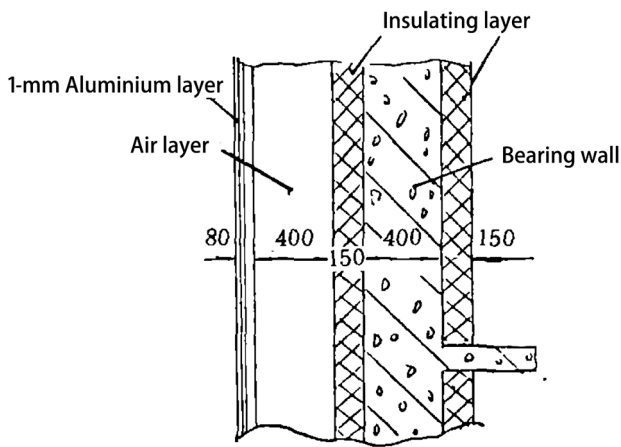


Fig. 2 The sectional drawing of the three layers cylindrical wall.

diameter of 23 m. The width of the slit is 5 m. This mechanical model was generated over a 3D SolidWorks model based on the engineer collection of 2.16-m telescopes.² The CFD model was imported from SolidWorks, using Ansys Fluent software to make the simulations. The size of fluid domain is about 100 m × 45 m × 43 m, ensuring the visibility of the tendency of airflow around the dome.

2.2 Computational Fluid Dynamics Configuration

The Reynolds (Re) number is an important dimensionless quantity in fluid mechanics used to help predict flow patterns in different fluid flow situations; it is defined as³

$$Re = \frac{uL}{\nu}, \quad (1)$$

where u is the velocity of the fluid with respect to the object (m/s), ν is the kinematic viscosity of the fluid (m^2/s), and L is the characteristic linear dimension. According to the weather station data at Xinglong Observatory, wind speed is usually 1 to 2 m/s during the observing nights. For 2.16-m telescope, characteristic length depends on the diameter of the dome. Thus, Re is over 1.66×10^6 and turbulent flow occurs around dome. The aerodynamic model is a transient problem, results after 4000 s of simulation are given in this paper. Pressure-based solver and $k-\epsilon$ model are used to simulate the incompressible airflow at low speed, which are also used by thirty meter telescope.⁴ The initial value for the ambient temperature is set as 278 K. The boundary conditions in CFD model are shown in Table 1.

2.3 Aerodynamic Performance

This CFD model simulates turbulent air flow of 1 m/s with the telescope and dome in two different orientations relative to wind: pointing parallel to the wind (slit to wind angle is 0 deg) and pointing perpendicular to the wind (slit to wind

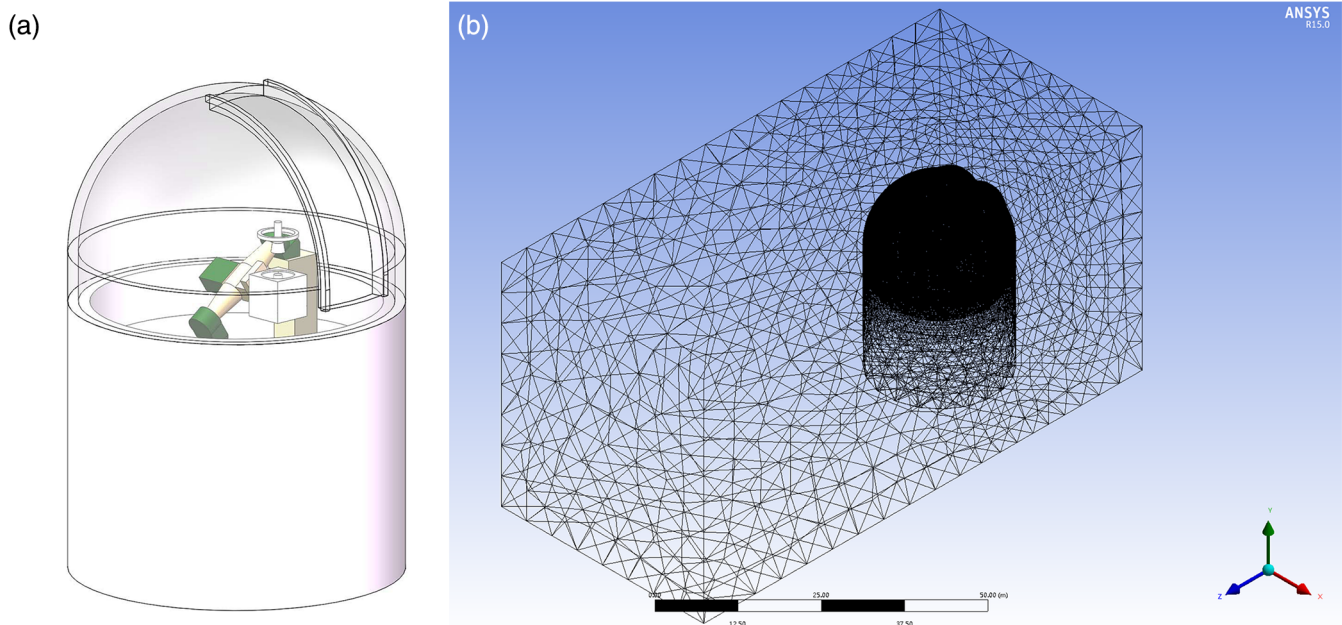


Fig. 3 (a) SolidWorks model and (b) CFD model of 2.16-m telescope.

Table 1 2.16-m telescope–dome CFD boundary conditions.

Surface	Temperature (K)	Type
Inlet	273	Velocity
M1	278	Wall
Floor	276	Wall
Dome surface	276	Wall
Outlet	273	Outflow
Top of the fluid domain	—	Symmetry
Sides of the fluid domain	—	Symmetry

angle is 90 deg). Two cross sections are defined in fluent to quantify the aerodynamic performance. As shown in Fig. 3, one of them is the intersection plane along the middle of the slit (black square), the normal vector of which is z axis. The other is a cross section with the normal vector of y axis (blue square). The red axis describes the orientation of the domain. The green arrow shows the direction of wind.

Case 1: Wind parallel to the slit. As shown in Fig. 4, the green arrow shows the direction of wind. Four contour maps are velocity magnitude, vector, turbulent kinetic energy, and turbulent intensity. The vector diagram is zoomed in for easy check (in red square). Turbulent kinetic energy is the measurement of turbulent intensity and is directly related to the transportation of momentum, heat, and moisture inside the boundary layer. According to Eq. (1), the wind speed is proportional to the Re number. When the velocity is large, the Re of air also becomes larger. The flow distribution diagrams (velocity and vector contours map) show the eddying of air in the upper edge of the open slit, which could cause air turbulent along the light path if telescope points to zenith. The max wind speed around the upper slit is 1.2 m/s while 0.6 m/s inside the dome. The turbulent intensity here is 37.6%. M2 is the nearest part to the slit, thus the turbulent kinetic energy and intensity values are larger than

other parts, showing “warmer” color. The air blown through the slit will form a vortex at the leeward corner (left of the mount), because there is no exit for the airflow to leave the dome (velocity vector). But this area is far from the light path and the turbulent kinetic energy is only $9.4 \times 10^{-5} \text{ m}^2/\text{s}^2$, not enough to cause major concern or reduce the image quality.

Case 2: Wind perpendicular to the slit. Figure 5 describes the wind orientation (in green arrow) and the coordinate system (in red) of case 2. The auxiliary cross-section planes are the same as case 1 (not shown in Fig. 5). Compared with case 1, the dome has a rotation angle of 90 deg counterclockwise and the fluid field does not change, noting that the coordinate system is different from case 1. As can be seen in Fig. 6, the wind direction is from left to right. In this case, the airflow is blocked by the windward wall of dome and flows to two sides of the dome, which produces the max wind speed (1.9 m/s) around the slit. Thus, image quality will be damaged because of the strong turbulent intensity (29.9%). There is no wind blowing directly into the dome, but several vortices can be seen at the left area of the mount. The max speed inside the dome is 0.8 m/s, larger than the max speed of case 1 as shown in Fig. 7. Some data of case 1 and case 2 are shown in Table 2. Turbulent kinetic energy and intensity data are presented at the surface of primary mirror, which is crucial in light path. The turbulent intensity values for case 1 and case 2 are approximate to the turbulent intensity in free atmosphere. The local atmosphere cannot be more stable through manual intervention, but we may use ventilation system and dome vents to reduce the turbulent intensity inside dome, achieve good dome seeing.

2.4 Temperature Inside the Dome

Temperature variation may change the air refractivity and then lead to turbulence airflow. Therefore, the temperature distribution inside the dome is another key point in the dome seeing study. Figure 8 shows the temperature distribution in the cross section along the slit at 100 s. Two different wind speeds have been used to simulate the effective of velocity. The left two images of Fig. 8 are for wind speed 1 m/s and the right two images for 2 m/s. The heat above the primary mirror could be removed away by wind. Temperature of primary mirror

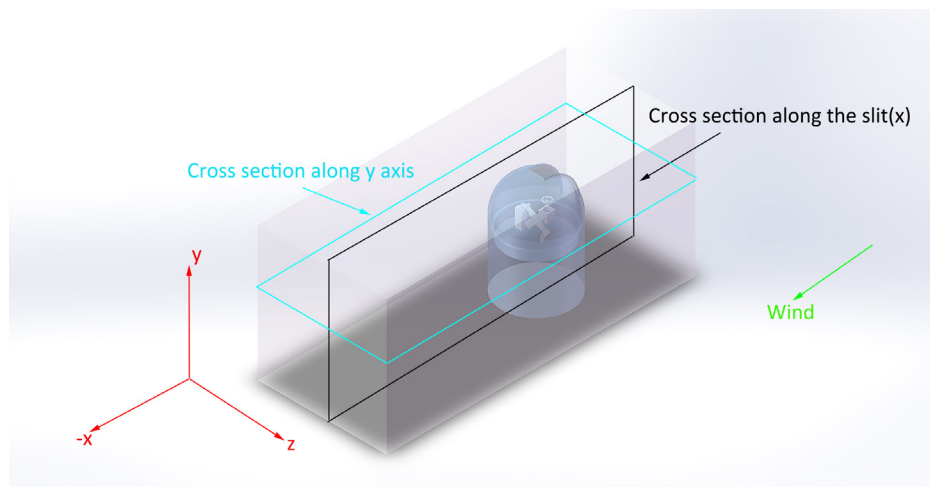


Fig. 4 The orientation information of the case: pointing parallel to the wind (slit to wind angle is 0 deg). The green arrow shows the wind direction, and the orientation of the model is described by the coordinate system in red. Two cross sections are orthogonal.

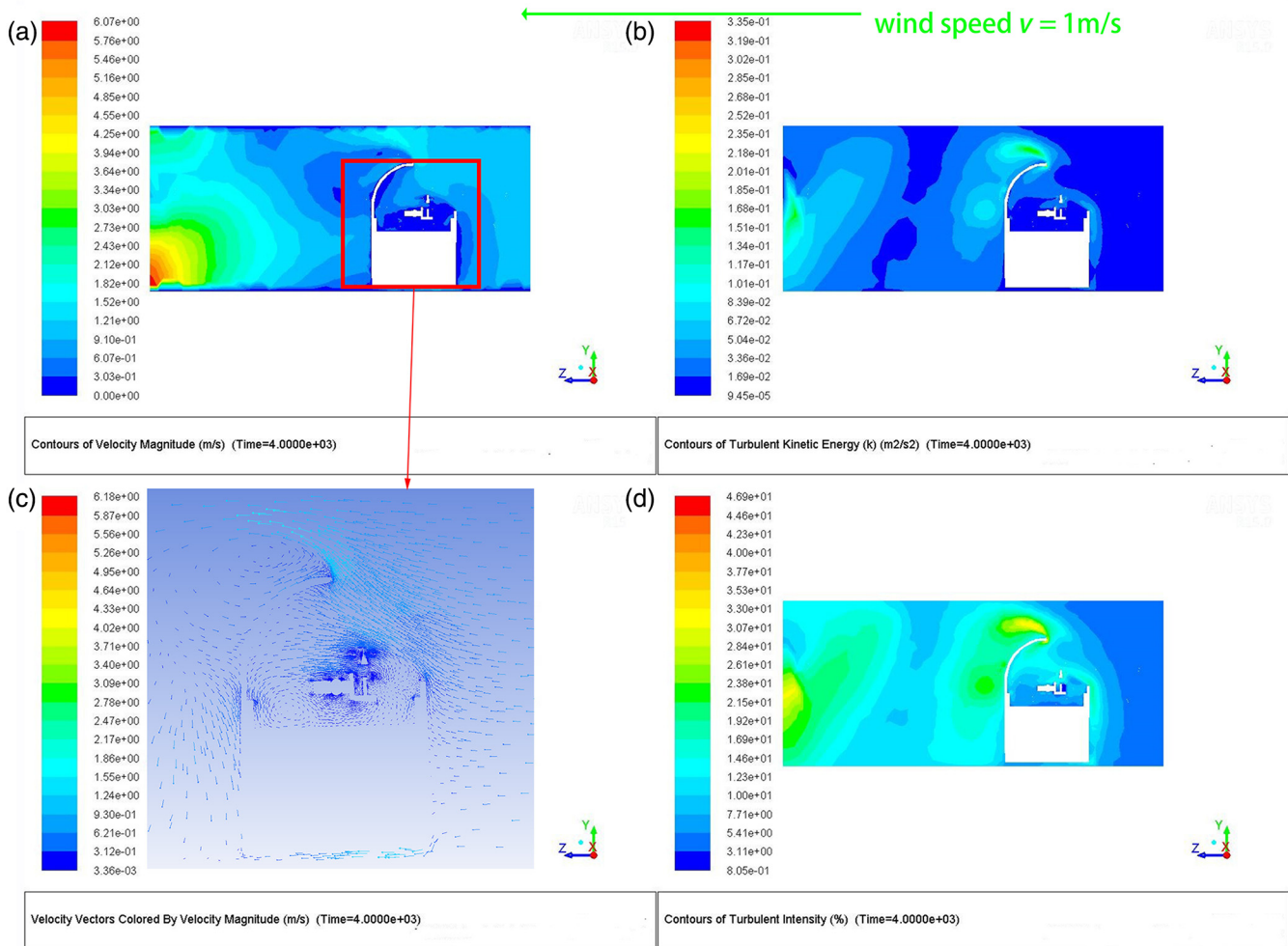


Fig. 5 Contour maps for the case 1: wind parallel to the slit, (a) velocity magnitude and (c) vector; (b) turbulent kinetic energy and (d) turbulent intensity.

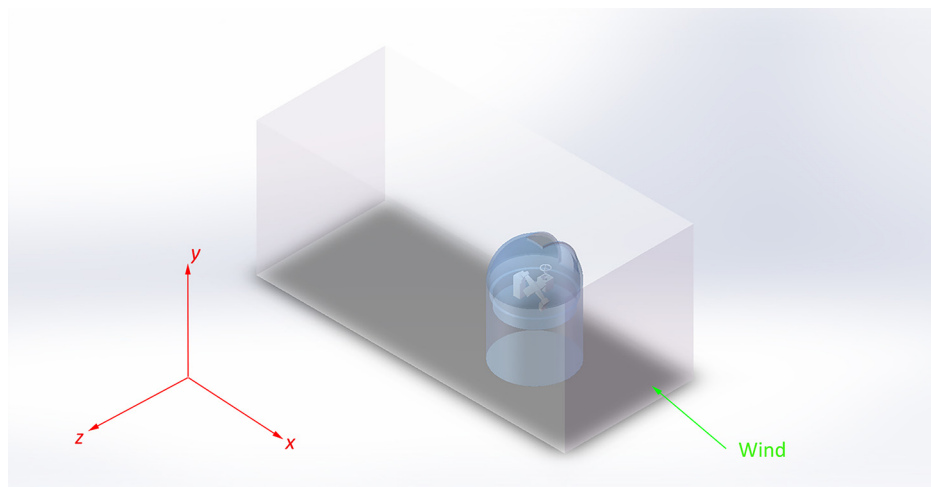


Fig. 6 The orientation information of the case: pointing perpendicular to the wind (slit to wind angle is 90 deg). The green arrow shows the wind direction, and the orientation of the model is described by coordinate system in red. Two auxiliary cross sections are the same as case 1.

for Fig. 8(b) is 276 K while Fig. 8(a) is still 278 K. This could be seen from both cross sections. Due to the single-slit type of the dome, turbulent air can only be removed through the slit where the fresh air comes in, an inefficient way of heat balance.

The frequency of air changes is only 4 to 6 times/h. In contrast, Large Synoptic Survey Telescope (LSST) has a series of vents to exhaust the air, about 150 air changes/h even the size of LSST's dome is larger than 2.16 m (30 m in diameter).⁵

Table 2 Aerodynamic performance for case 1 and case 2.

Parameter	Case 1	Case 2
Max speed inside the dome (m/s)	0.61	0.83
Turbulent kinetic energy ($\text{k} \cdot \text{m}^2/\text{s}^2$)	0.01	0.02
Turbulent intensity (%)	5.41	10.73

The full width half maximum (FWHM), θ , is computed using the functions derived by Blanco, Zago, Kolmogorov, Tatarskii⁶⁻¹¹

$$D_T = \langle [T(r) - T(r + \Delta r)]^2 \rangle = C_T^2 \Delta r^2 / 3, \quad (2)$$

$$C_n^2 = C_T^2 \left[77.6 \times 10^{-6} (1 + 7.52 \times 10^{-3} \lambda^{-2}) \frac{P}{T^2} \right]^2, \quad (3)$$

$$r_0 = \left[0.423 \left(\frac{2\pi}{\lambda} \right)^2 (\cos \gamma)^{-1} \int_{\text{Vertical}} C_n^2(y) dy \right]^{-3/5}, \quad (4)$$

$$\theta = 0.975863 \frac{\lambda}{r_0}, \quad (5)$$

where D_T is the structure function, C_T^2 is the temperature structure coefficient, Δr is the separation, P is the pressure (mb), T is the ambient temperature (K), r_0 is the Fried parameter, and y is the height from primary mirror. For a vertical direction zenith distance $\gamma = 0$ deg and $\lambda = 500$ nm at Xinglong Observatory (pressure $P = 90125$ Pa = 901 mb), the FWHM is expressed as

$$\theta = \frac{8.418 \times 10^5}{T^{2.4}} \left[\int_H C_T^2(y) dy \right]^{3/5}. \quad (6)$$

According to the above equation, the dome seeing can be calculated by monitoring the temperature at different heights above the primary mirror. The 42 symmetrical temperature monitoring points locate above the primary mirror in CFD ($y = 0$ to 14 m, $\Delta r = 1.5$ m), as shown in Fig. 9.

The temperature data are recorded at different wind speeds ($v = 1$ and 2 m/s) and different times (100 and 600 s) for case 1 and case 2. The ambient temperature T is set to 273 K. Table 3 shows the calculated dome seeing for case 1 and case 2. For a faster wind speed ($v = 2$ m/s), dome seeing is larger at 100 s but lower at 600 s, because the quick heat balance rate. Due to

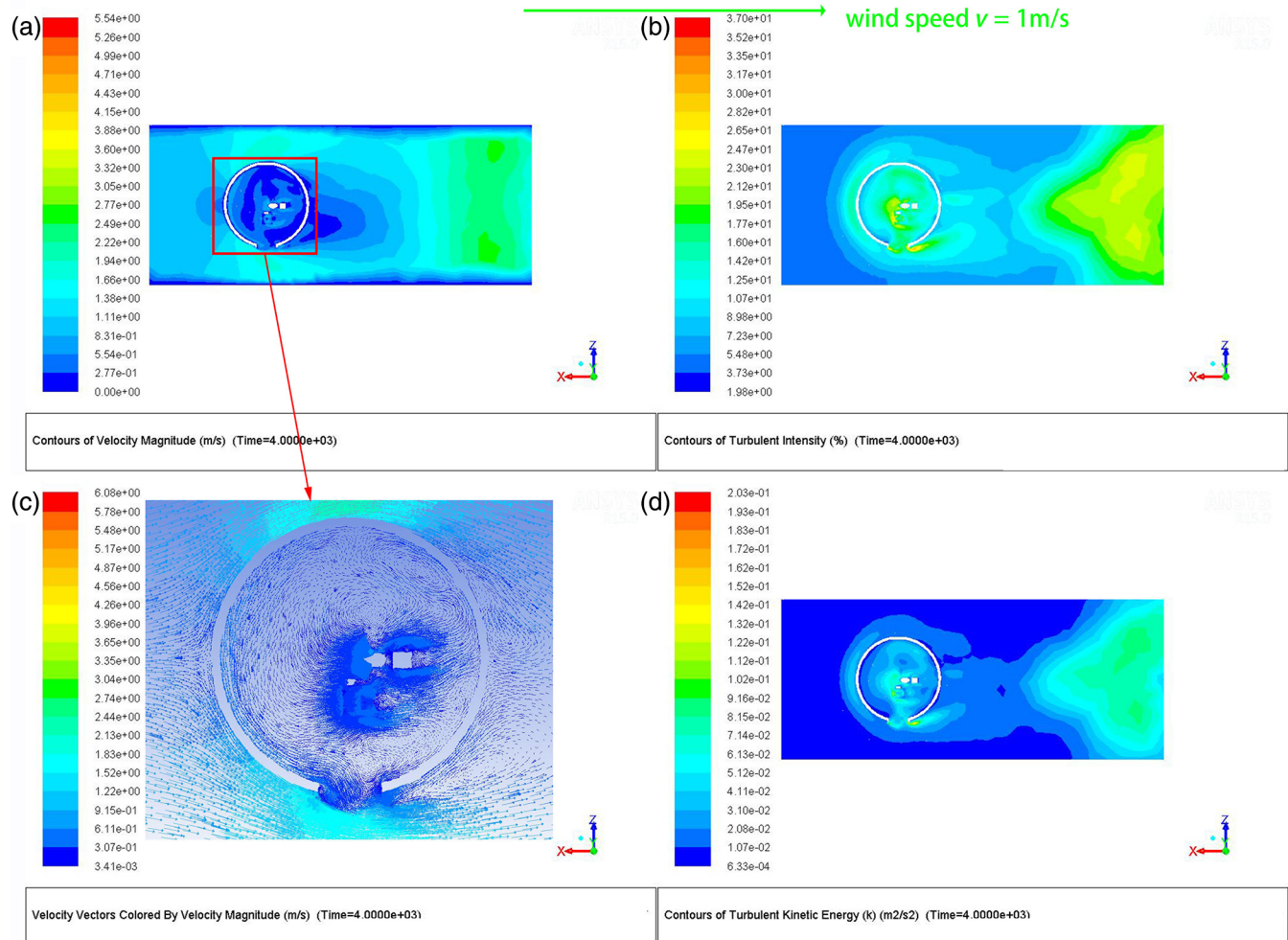


Fig. 7 Contour maps for the case2: wind perpendicular to the slit, (a) velocity magnitude and (c) vector; (b) turbulent intensity and (d) turbulent kinetic energy.

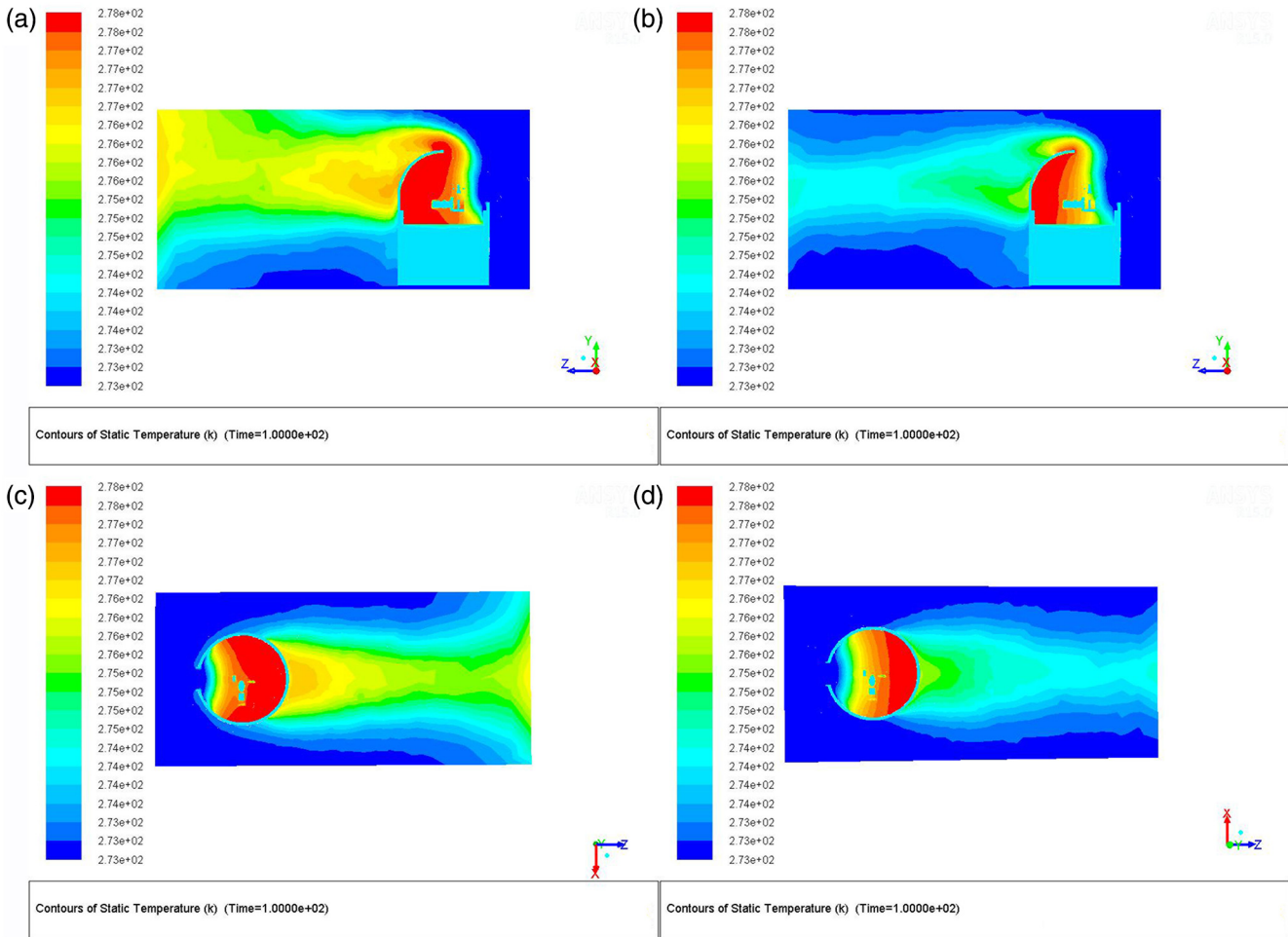


Fig. 8 Temperature contour at 100 s; (a) and (c) wind speed = 1 m/s; and (b) and (d) 2 m/s, from two directions: along (a and b) the slit and along (c and d) y axis.

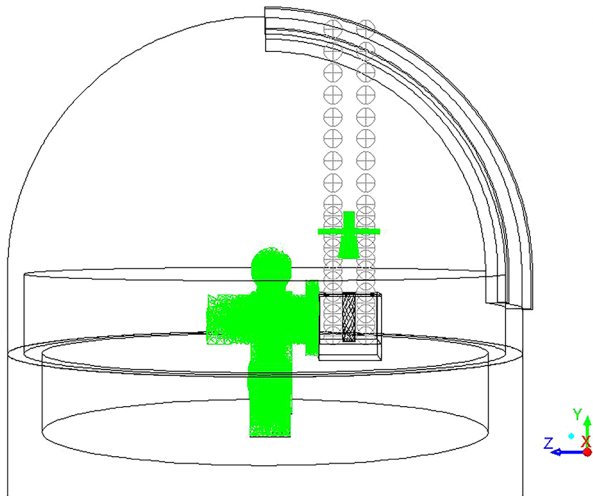


Fig. 9 Monitoring points distribution (shown as “+”); horizontal distance (z) for two points is 1.5 m and perpendicular distance (y) is 0 to 14 m from M1 surface.

the different wind-slit angles, the dome seeing for case 1 is quite smaller than that for case 2. The results give us a venting strategy that the dome vents should be parallel to the wind direction, i.e., open the vents that face to the wind.

Table 3 Dome seeing for case 1 and case 2.

	$v = 1100 \text{ s}$	$v = 1600 \text{ s}$	$v = 2100 \text{ s}$	$v = 2600 \text{ s}$
FWHM_Case 1	0.33"	0.14"	0.52"	0.03"
FWHM_Case 2	1.14"	0.59"	2.54"	0.30"

3 Conclusions

CFD simulations have provided a method to determine the aerodynamic and thermal performance of 2.16-m telescope to meet the image quality requirements by a thorough study in dome seeing. The image quality through the telescope is critically affected by dome seeing, as can be concluded from the CFD data. The dome seeing comparison shows the wind-slit angle is an important factor and gives us a strategy for a venting system. In future work, the venting system will be designed and the differential image motion monitor (DIMMs) will play a role in dome seeing monitoring. Two or three DIMMs will be needed to compare seeing outside the dome with that inside the dome. However, dome seeing measurements have several difficulties, including concurrent observation and the dome seeing relationship with wind direction, slit to wind angle, and ambient temperature.

Acknowledgments

This work was supported by the National Natural Science Foundation of China (NSFC) (Grant Nos. 11703043 and U1831209). We thank Feng Xiao, Junjun Jia, Yunpeng Wang, and Sen Liu for providing the guidance of 2.16-m telescope operation.

References

1. Z. Fan et al., “The Xinglong 2.16-m telescope: current instruments and scientific projects,” *Publ. Astron. Soc. Pac.* **128**, 115005 (2016).
2. D. Su, *2.16-m telescope work collections*, Science and Technology of China Press, Beijing (2001).
3. S. Arnold, “A contribution to hydrodynamic explanation of turbulent fluid motions,” in *Int. Congr. Mathematicians*, Vol. 3, pp. 116–124 (1908).
4. K. Vogiatzis and G. Z. Angeli, “Strategies for estimating mirror and dome seeing for TMT,” *Proc. SPIE* **6271**, 62710O (2006).
5. D. R. Neill, J. D. Barr, and V. L. Krabbendam, “Initial design factors and airflow analysis for the LSST enclosure,” *Proc. SPIE* **7017**, 70170P (2008).
6. D. R. Blanco, “Effects of air pressure, temperature, and relative humidity on seeing,” *Proc. SPIE* **4004**, 552–558 (2000).
7. L. Zago, “The effect of the local atmospheric environment on astronomical observations,” Thesis No 1394, Ecole Polytechnique Federale de Lausanne (1995).
8. L. Zago, “Engineering handbook for local and dome seeing,” *Proc. SPIE* **2871**, 726–736 (1997).
9. A. N. Kolmogorov, “The local structure of turbulence in incompressible viscous fluid for very large Reynolds numbers,” in *Proc. Math. and Phys. Sci.*, Vol. 434, pp. 9–13 (1991).
10. V. I. Tatarskii, *Wave Propagation in Turbulent Medium*, McGraw-Hill, New York, p. 285 (1961).
11. D. L. Fried, “Statistics of a geometric representation of wavefront distortion,” *J. Opt. Soc. Am.* **55**(11), 1427–1431 (1965).

Taoran Li received his PhD from the National Astronomical Observatories, Chinese Academy of Sciences (NAOC) in 2016. Since 2016, he has been an exchange scholar for one year at Isaac Newton Group of Telescopes, La Palma, Spain. He has been an optical engineer at NAOC (from 2016 to till date). His research interests are stray light analysis and control for astronomical telescopes, air turbulence simulation by CFD, 3D structure modeling and analysis, and telescope assembly and alignment.

Biographies of the other authors are not available.